Effects of process conditions on the chemistry of an Ar/C2H2 dust-forming plasma

Igor Denysenko, Erik von Wahl, Safa Labidi, Maxime Mikikian, Holger Kersten, Titaïna Gibert

DOI: 10.1002/ppap.201800209

Article type: Full Paper

Effects of Process Conditions on the Chemistry of an Ar/C_2H_2 Dust-Forming Plasma

Igor B. Denysenko*, Erik von Wahl, Safa Labidi, Maxime Mikikian, Holger Kersten, Titaïna Gibert

_____

Prof. I. B. Denysenko

School of Physics and Technology, V. N. Karazin Kharkiv National University,

4 Svobody sq. 61022, Kharkiv, Ukraine

E-mail: idenysenko@yahoo.com

E. von Wahl, S. Labidi, Dr. M. Mikikian, Dr. T. Gibert

GREMI, UMR7344 CNRS/Université d'Orléans, Orléans, F-45067, France

E. von Wahl, Prof. H. Kersten

Institut für Experimentelle und Angewandte Physik, Christian-Albrechts-Universität zu Kiel, Kiel, 24098, Germany

A volume-averaged model and numerical simulations are used to clarify the effects of process conditions on the plasma chemistry and species initiating the formation of nanoparticles in an Ar/C_2H_2 plasma. It is shown that Ar/C_2H_2 plasmas with low electron density, moderate input flux of acetylene and an electron energy distribution function (EEDF) close to the Druyvesteyn EEDF are the most suitable for the production of carbonaceous nanoparticles. These results are verified by a direct comparison with experimental data and enable to formulate recommendations for future experiments with a controlled growth of nanoparticles in chemically-active plasmas.

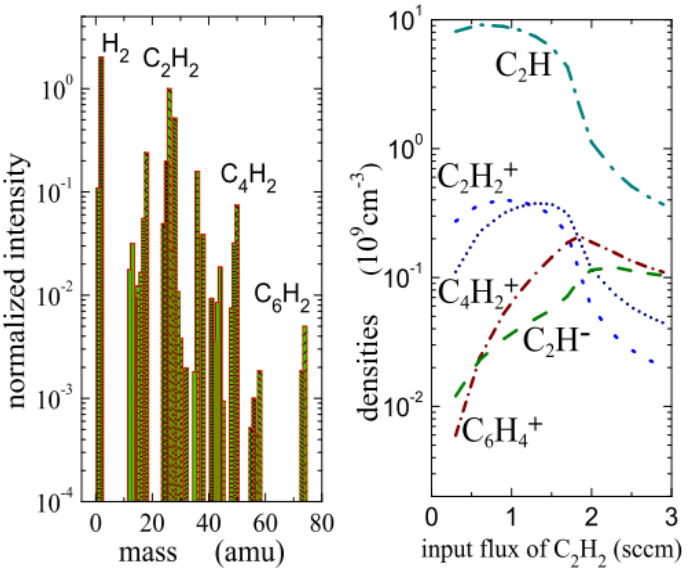

Keywords: computer modeling; hydrocarbons; ion-assisted chemistry; mass spectrometry; nanoparticles

1. Introduction

Plasmas with nano- and micrometre-sized particles (dust particles) are useful for various applications[1–5] and are also of great fundamental interest.[6–10] The dust particles can either be injected into laboratory plasmas from outside or can grow inside due to different chemical reactions. For example, formation of carbonaceous dust particles takes place in reactive plasmas operating in mixtures of different gases with methane, acetylene or ethylene.[11–13]

In the past two decades, plasmas used for the formation of carbonaceous dust particles have been intensively investigated both by experimental measurements[11–21] and numerically.[21–28] The experiments have shown that dust particle growth strongly depends on the concentrations of C_2H^- ions, which are supposed to act as a main species for the initiation of dust formation,[11] and C_2H neutral radicals.[16] The experiments also revealed that the formation of dust particles in Ar/C_2H_2 plasmas is accompanied by a decrease of the electron and acetylene densities and by an increase of the electron temperature and the density of metastable argon atoms.[16-20] Numerical simulations of the nucleation of nanoparticles in C_2H_2 and Ar/C_2H_2 plasmas showed that positive and negative ions, as well as hydrocarbon radicals may take part in the initial stage of particle formation.[22–27]

The experiments on nanoparticle growth have also revealed that the growth is possible only at certain process conditions (pressure, discharge power, input gas fluxes, etc.). Varying the conditions can affect the internal plasma parameters as the electron, ion and neutral densities and the electron energy distribution function. To initiate the nanoparticle formation, certain internal conditions are required. In particular the densities of species taking part in the nucleation of nanoparticles should be above threshold values.[16]

However, in most numerical studies on plasmas used for the formation of carbonaceous nanoparticles, it was not analysed how different process conditions affect the species which may initiate nanoparticle growth (negative and positive hydrocarbon ions and hydrocarbon radicals), while in most experiments, the process conditions suitable for

nanoparticle formation have been chosen empirically. To control the dust particle growth, a fundamental understanding of the involved chemical processes and the role of process conditions on species initiating the nanoparticle growth have to be revealed.

In this paper, we analyse how the properties of an Ar/C_2H_2 plasma (the ion, electron and neutral particle densities, the electron temperature and the dust charge) depend on several key process conditions: discharge power, acetylene input flux, shape of the electron energy distribution function and nanoparticle density. Moreover, processes responsible for the production and loss of different ions and neutrals in the discharge are analyzed, in order to identify the most important ones. The numerical study is carried out for process conditions similar to our experiments on nanoparticle growth[21,29] using a global (volume-averaged) model. The 0D model approach has shown to be effective for the analysis of chemically-active gas dischargers at low pressures.[30–32] Finally, we discuss, which process conditions are the most suitable for nanoparticle genesis.

2. The Model

The model considers an Ar/C_2H_2 plasma of R = 22 cm radius and L = 32.4 cm height sustained in a cylindrical stainless steel chamber as in the experiment of interest.[21,29] To analyze the plasma properties, a volume-averaged model is used assuming that the plasma consists of electrons with density n_e, nine positive ions ($C_2H_2^+$, Ar^+, ArH^+, H_2^+, H^+, $C_4H_3^+$, $C_4H_2^+$, $C_6H_4^+$ and $C_2H_3^+$), four nonradical neutrals (Ar, C_2H_2, H_2 and C_4H_2), two radicals (C_2H and H), metastable argon atoms (Ar_m) with density n_m, argon atoms in the resonance 4s states ($^3P_1$ and $^1P_1$) (Ar_r) with density n_r as well as argon atoms in 4p states (Ar(4p)) with density n_{4p} and negatively charged dust particles with density n_d, radius a_d and charge Z_d (in units of electron charge e). In the 0D model, densities n_m, n_r and n_{4p} represent composite levels of: $^3P_0$ and $^3P_2$ (metastable), $^3P_1$ and $^1P_1$ (resonance) and 4p states, respectively. The model takes into account the most important neutral species and positive ions evidenced in

our experiments on nanoparticle growth in an Ar/C_2H_2 plasma (**Figure 1**). The details of the experiments can be found elsewhere[21,29]

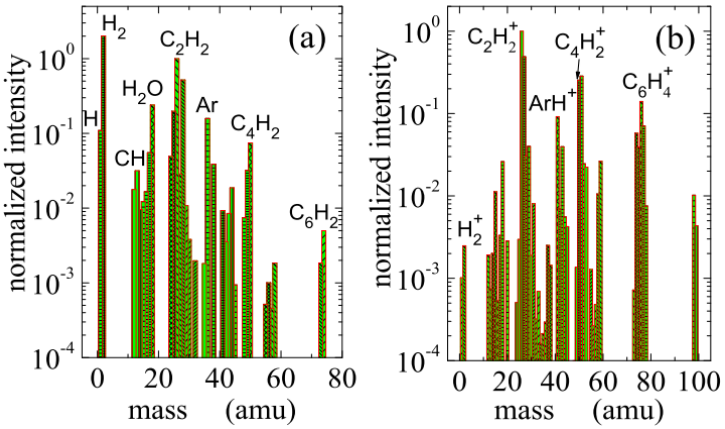

Figure 1. Mass spectra for neutral species (*a*) and positive ions (*b*) measured in our experiments on growth of nanoparticles for the growth time when the dust radius is nearly 25 nm. The Ar/C_2H_2 plasma discharge was driven at 13.56 MHz and a radio-frequency power of 9 W. The plasma height L and radius R were nearly 32.4 cm and 22 cm, respectively. Acetylene with the flux Q_{C2H2}=1.5 sccm and argon with the flux Q_{Ar}=11 sccm were used as a reactive precursor and a background gas, respectively. The process gas pressure in the reactor was about 4.2 Pa.

The dominant neutral species are argon atoms with their density $n_{Ar} \approx P/(k_B T_g) \approx$ 1.01×10^{15} cm^{-3}, with P = 4.2 Pa is the pressure of argon gas, k_B is the Boltzmann constant and T_g is the gas temperature considered to be 300 K. Note that in our mass spectra measurements[21] we were not able to measure intensities of argon ions and neutrals at mass 40 amu simultaneously with other species because the intensity was much above saturation and the instrument would shut down. We assume that the energy distribution for ions is Maxwellian, and that ions and dust particles are at gas temperature. We also assume that the plasma contains negative ions C_2H^- with density n^- although not measured in our experiment

due to mass spectrometer limitations and complexity in extracting negative ions from the positive plasma glow. At large ratio of the argon atom density to that of acetylene molecules, the anions C_2H^- are the dominant negative ions.[26,27]

In the model, the electron energy distribution function (EEDF) is allowed to vary according to the general distribution function given by[31,33]

$$F(\varepsilon) = A_1 \varepsilon^{1/2} \exp(-A_2 \varepsilon^x), \tag{1}$$

where ε is the electron energy and x is a number with $x = 1$ or $x = 2$ for Maxwellian or Druyvesteyn electron energy distributions, respectively. The coefficients A_1 and A_2 are functions of the number x and average electron energy[31,33] $\langle \varepsilon \rangle = \int_0^\infty \varepsilon F(\varepsilon) d\varepsilon = \frac{3}{2} e T_{\text{eff}}$, where T_{eff} is the effective electron temperature. The EEDF has the following normalization $\int_0^\infty F(\varepsilon) d\varepsilon = 1.$

The plasma is assumed to be quasineutral, or

$$\sum_\alpha n_\alpha^+ = n_e + n^- + |Z_d| n_d, \tag{2}$$

where n_α^+ is the density of the α-th positive ion species.

The volume-averaged model consists of the particle balance equations for ions and neutrals, the power balance equation and the equation for the dust charge. In this study, we consider various processes for the generation and loss of the discharge species, including collisional processes in the bulk plasma, processes on the plasma walls and dust particles, as well as pumping gas in and out of the chamber. In the power balance, we accounted for the power loss due to electron-neutral collisions and the losses due to charged particle fluxes to the walls and dust particles. The electron-molecule (atom) and ion-molecule (atom) processes, the reactions for neutral-neutral collisions, the details concerning the model equations, as well

as the numerical method of their solution are described in detail in the Supporting information and can also be found in ref.[21]

3. Results of Calculations and Discussion

Using the volume-averaged model, we have analyzed how the Ar/C_2H_2 plasma properties depend on different process conditions (absorbed power, EEDF, input flux of C_2H_2 and nanoparticle density). The study has been carried out for the conditions similar to our experiments on nanoparticle growth.[21] Main processes responsible for the generation and loss of different ions and neutral species have also been analysed and are presented in the Supporting information. In most cases studied here, the EEDF is considered to be Druyvesteyn-like as it is typical for radio-frequency laboratory plasmas at $n_e < 10^{11}$ cm^{-3} and $Pd > 0.2$ Torr×cm,[34] where $d \approx L/2$ is the dimension of reactor in cm, i. e., for the conditions of our experiments.[21,29] As grown nanoparticles may affect the EEDF[35,36], the study of its variation on the plasma properties is also of particular interest.

3.1. Effects of Variation in Discharge Power on the Densities of Ions and Neutral Species

First, we analyze how the properties of an Ar/C_2H_2 plasma depend on the absorbed power P_{abs}. An increase of P_{abs} leads to an elevation in the electron density (**Figure 2a**), while the electron temperature only slightly depends on a power variation and remains at $T_{eff} \approx 3$ eV.

The increase of n_e at increasing P_{abs} is accompanied by an increase of the densities of excited argon atoms Ar* (Figure 2a) and the densities of Ar^+, $C_2H_2^+$, $C_4H_3^+$, $C_4H_2^+$, ArH^+, H^+, H_2^+, $C_6H_4^+$ (only for $P_{abs} < 7$ W) and $C_2H_3^+$ (only for $P_{abs} < 10$ W) (Figure 2b,c) because of an increasing number of electron-neutral collisions involving argon atoms and nonradical molecules. The $C_2H_3^+$ and $C_6H_4^+$densities decrease for large P_{abs} (Figure 2b,c) due to the disappearance of the nonradical molecules C_2H_2 and H_2 ($C_2H_2^+ + H_2 \rightarrow C_2H_3^+ + H$, $C_4H_2^+ + C_2H_2 \rightarrow C_6H_4^+$) (Figure 2d).

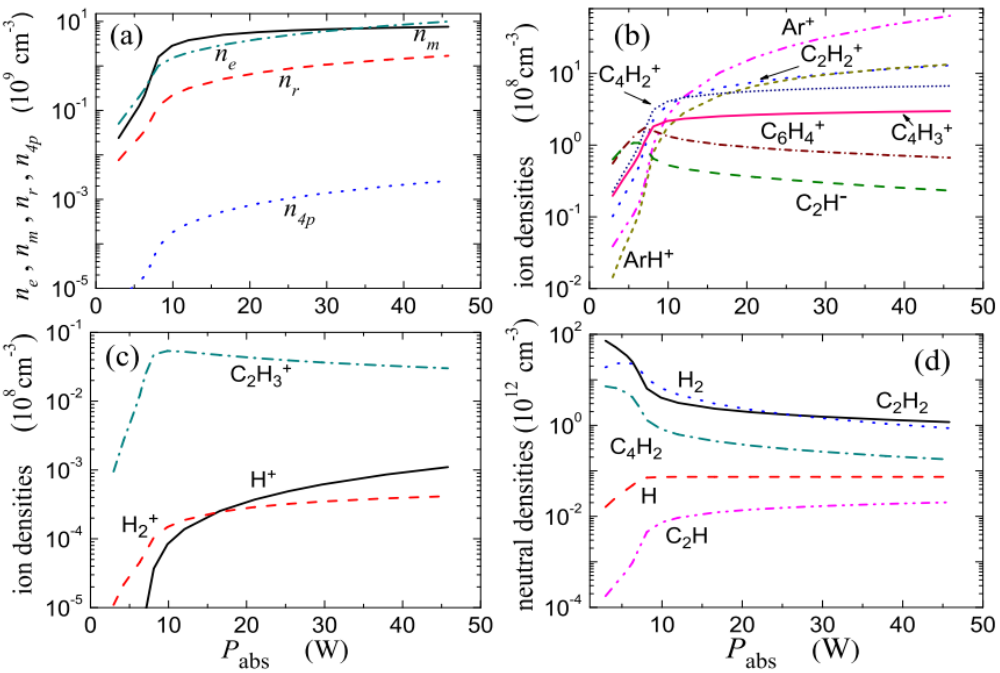

Figure 2. The densities of electrons and argon atoms in excited states (*a*), ions [(*b)* and (*c*)] and neutral species (*d*) as functions of the absorbed power. The dependencies are obtained for Q_{C2H2}=1.5 sccm, Q_{Ar}=11 sccm, x = 2, L= 32.4 cm, R = 22 cm and n_d = 0.

Indeed, with the increase of the discharge power, densities of C_2H_2, C_4H_2 and H_2 (H_2 only for P_{abs} > 5.6 W) decrease as they are mainly lost in collisions with electrons, positive ions, C_2H radicals and argon atoms in different excited states (see the Supporting information). The density of H_2 slightly increases at small absorbed powers (P_{abs} < 5.6 W) due to an increase of the H density as H_2 is mainly produced by collisions of H with the walls.

The H atoms are mainly generated by electron-impact dissociation and ionization of H_2, in collisions of Ar* with C_2H_2, C_4H_2 and H_2 and in collisions of C_2H with C_2H_2 and H_2 (see the Supporting information). Due to an enhancement of these production processes, the H density becomes larger with increasing P_{abs} for P_{abs} < 10 W. For larger absorbed powers, production and loss processes counterbalance, leading to a nearly constant H concentration. The density of C_2H radicals grows with increasing P_{abs} because of the also growing Ar*

concentration (C_2H is mainly produced in collisions between C_2H_2 molecules with electrons and Ar* atoms) and because of the decrease in C_2H_2 density (C_2H is mainly lost in collisions with acetylene molecules).

Finally, it can be seen, that the C_2H^- concentration is growing with P_{abs} for low absorbed powers (P_{abs} < 5.6 W) but then descending for high P_{abs}. This originates from the interplay of an enhancement of the C_2H^- production in collisions between electrons with C_2H_2 on one hand and an enhancement of anion losses in collisions with positive ions and hydrogen atoms (see the Supporting information) on the other hand.

For the experimental conditions (n_e =1.28×10^9 cm^{-3}, P_{abs} = 9 W), the simulation shows that the dominant neutrals in the plasma are Ar, C_2H_2 and H_2, while the dominant ions are Ar^+, $C_2H_2^+$, $C_4H_2^+$, $C_4H_3^+$, $C_6H_4^+$ and ArH^+. The densities of H_2^+ and H^+ are essentially smaller than those of other ions. This agrees well with our measurements of mass spectra for neutral species and positive ions for plasmas largely affected (Figure 1) and little affected by the nanoparticle presence.[21] Therefore, the model description of the reactive chemistry can generally be regarded as valid with the ability to reproduce experimental trends qualitatively.

To summarize, under our experimental conditions (i.e. P_{abs} ~ 9 W), we find a relatively large amount of all the species taking part in the initial stage of nanoparticle formation:[16,23,25] C_2H^- (~ 10^8 cm^{-3} as in ref.[25]), C_2H (~6.0×10^9 cm^{-3}) and most of the reactive positive ions (for example, the density of $C_6H_4^+$ is 1.4 ×10^8 cm^{-3}). Therefore, our power regime may be favorable for nanoparticle nucleation.

3.2. Effects of Variation in Shape of the Electron Energy Distribution Function

In the following, we will analyse how the plasma properties depend on the EEDF shape that can for example be influenced by the choice of plasma source. For that, we will vary the parameter x in Equation (1), while other process parameters remain fixed.

In **Figure 3a,b**, the effective electron temperature and the densities of electrons and metastable argon atoms as functions of x are shown. One can see that n_m and T_{eff} are increasing with x, while the electron density drops. The correlation between T_{eff} and x comes from a more convex electron energy probability function (EEPF), $F(\varepsilon)/\varepsilon^{1/2}$, and, as a result, the number of electrons in the energy range $3\ \text{eV} < \varepsilon < 17\ \text{eV}$ grows with respect to their total number (Figure 3c). It is also accompanied by an increasing n_m (Figure 3a) and by an enhancement of the power loss per electron in various electron-neutral inelastic collisions. Because of the power loss enhancement, the electron density decreases (Figure 3b). Note that for a pure argon plasma, in ref.[33] it was also found that T_{eff} grows and n_e becomes smaller with an increase of x.

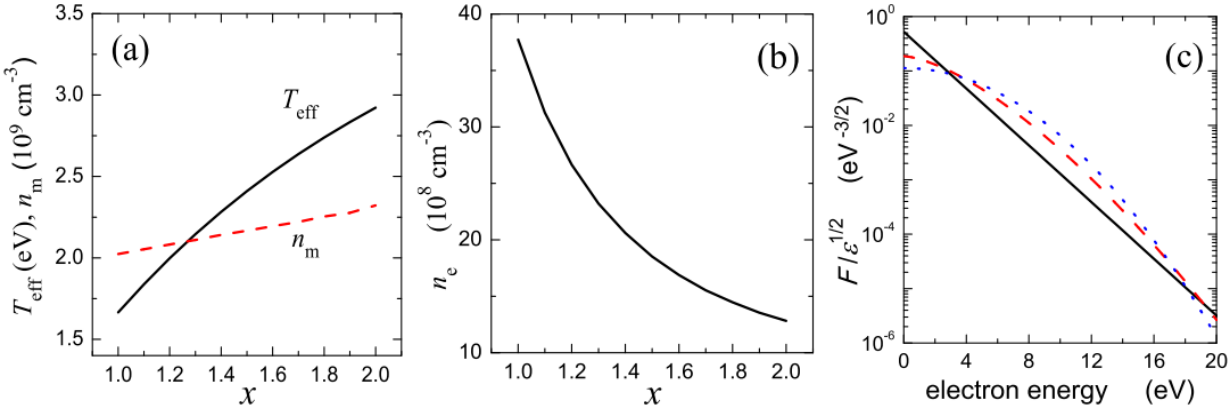

Figure 3. n_m (a), T_{eff} (a), n_e (b) as functions of x. c) The EEPFs for x = 1 (solid curve), x =1.5 (dashed curve) and x =2 (dotted curve). Here, T_{eff} = 1.67 eV, 2.41 eV and 2.92 eV for x = 1.0, 1.5 and 2.0, respectively. The dependencies are calculated for P_{abs} = 9 W and the other parameters are the same as in Figure 2.

As a result of the n_e reduction, the density of acetylene molecules is slightly enhanced for greater values of x (**Figure 4a**). This is accompanied by greater C_4H_2 and H_2 concentrations. Additionally, increasing the C_2H_2 density and n_m makes the reaction $Ar_m + C_2H_2 \rightarrow C_2H + Ar + H$ more probable, so that the C_2H density slightly grows with x. The amount of atomic hydrogen also grows with x. In our opinion, this is mainly due to an

enhancement of the H production in collisions of C_2H with C_2H_2 and of Ar* with C_2H_2, C_4H_2 and H_2 (see the Supporting information).

The densities of positive ions, however, drop with increasing x (Figure 4b) because of greater losses in collisions with neutral species, whose densities become larger, and because of a lower production in electron-neutral collisions (because of the n_e decrease). On the contrary, the density of C_2H^- slightly grows with x for $x \leq 1.3$ but then also slightly decreases at larger x. This dependence on x, in our opinion, is mainly due to a combination of losses in collisions with positive ions and H. At small x, the former process is dominant while at large x, the latter one takes over. Therefore, the maximum density of anions is found for moderate x values.

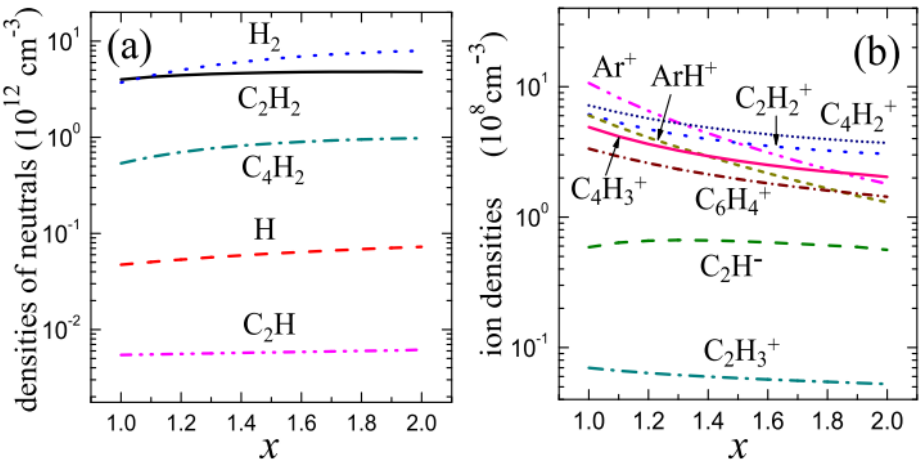

Figure 4. The densities of neutral species (a) and ions (b) as functions of x for the same conditions as in Figure 3.

3.3 Effects of Variation in Acetylene Input Flux

Next, we analyse how a variation of the C_2H_2 input flux affects the plasma properties and the chemical composition. An increase of Q_{C2H2} naturally leads to an elevation in the C_2H_2, H_2 and C_4H_2 densities (**Figure 5a**). Thus, the power losses by inelastic collisions of electrons with these molecules increase. As a result, for a fixed absorbed power (here, P_{abs} = 9 W) a

higher Q_{C2H2} causes a lower electron density (Figure 5c). Due to the small amount of electrons, the densities of excited argon atoms, including metastables, then decrease too (Figure 5c). With increasing Q_{C2H2}, the effective temperature slightly decreases from 2.96 eV up to 2.9 eV in the range 0.3 sccm $\leq Q_{C2H2} \leq$ 1.7 sccm and slightly increases at higher Q_{C2H2} (for example, T_{eff} = 3.12 eV for Q_{C2H2} = 2.9 sccm).

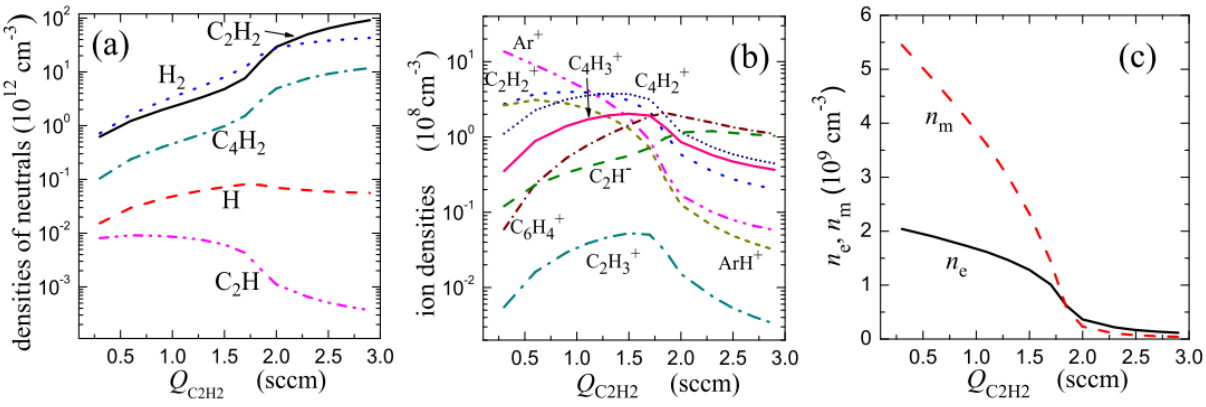

Figure 5. The densities of neutral species (a), ions (b), electrons (c) and argon atoms in the metastable states (c) as functions of the acetylene input flux. The dependencies are obtained for P_{abs} = 9W and the other external parameters are the same as in Figure 2.

Since the production and loss of ions and radicals in the Ar/C_2H_2 plasma depend on the electrons, Ar*, H_2, C_2H_2 and C_4H_2 densities, their Q_{C2H2} dependencies indirectly determine the ones for ions and radicals (Figure 5a,b). In particular, due to the reduction of n_e and n_m for higher Q_{C2H2}, the production and density of Ar^+ also decrease, in turn leading to the decrease in the ArH^+ density. At small Q_{C2H2}, the densities of positive hydrocarbon ions grow with Q_{C2H2} because of the C_2H_2 and C_4H_2 density increase (the ions are produced from these molecules). At large Q_{C2H2}, however, the hydrocarbon cation densities drop due to an enhancement of their losses in collisions with molecules, whose densities are growing at the same time, and due to a decrease of their production in collisions with electrons and Ar* (their densities are reduced).

For Q_{C2H2} < 2.3 sccm the density of C_2H^- anions grows with Q_{C2H2} due to the likewise growing C_2H_2 density and due to the reduction of the total density of positive ions (the anions are produced in collisions of electrons with acetylene molecules, while their loss is due to the collisions with positive ions and hydrogen atoms). At Q_{C2H2} > 2.3 sccm, the C_2H^- concentration slightly decreases with a further Q_{C2H2} increase because of the reduced electron density. Since the production of the C_2H radical mainly takes place in collisions of electrons and excited argon atoms with acetylene molecules, the decrease in electron and excited atom densities at increasing Q_{C2H2} is accompanied by a reduction of the C_2H density.

3.4. Effects of Variation in Dust Density

The formation of nanoparticles in the plasma may essentially affect the discharge properties due to the collection of electrons, ions and radicals by the dust particles. As a result, the electron density decreases and T_{eff} grows when n_d becomes larger (**Figure 6a,b**). In turn, due to the increase of T_{eff}, the density of metastable argon atoms also grows as long as the dust amount stays below $n_d < 3\times10^7$ cm^{-3} (Figure 6b). At $n_d > 3\times10^7$ cm^{-3}, n_m drops again because of a decrease in n_e. Furthermore, the increase in T_{eff} also enhances the production of Ar^+ in electron-atom collisions (Figure 6c). This is accompanied by an enhancement of the ArH^+ production in collisions of Ar^+ with H_2, and thus, leads to an increase in the ArH^+ density and to a decrease in the H_2 density (Figure 6d). As C_2H_2 is mainly lost in collisions with Ar* atoms, the C_2H_2 density evolves inversely to n_m. In turn, the C_4H_2 production is related to the C_2H_2 density,[17] and, as a result, the n_d - dependencies of both molecules are similar.

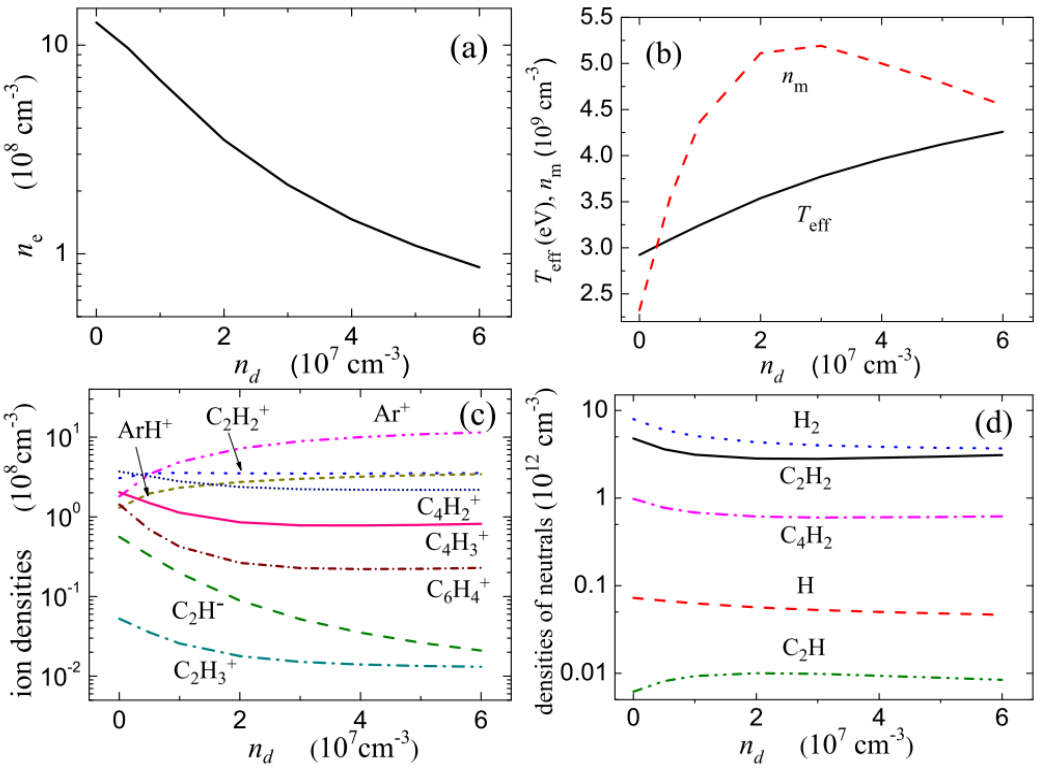

Figure 6. The density of electrons (a), n_m and T_{eff} (b), the ion densities (c) and the densities of neutral species (d) as functions of the dust density. The dependencies are calculated for a_d = 25 nm, Q_{C2H2} = 1.5 sccm and the other parameters as in Figure 5.

At large dust densities, the deposition on dust particles is the dominant loss process for most hydrocarbon ions (see the Supporting information) and their densities are smaller than in the $n_d = 0$ case. The concentration of negative ions C_2H^- becomes smaller for larger n_d mainly due to a reduction of the anion generation through electron attachment to C_2H_2 (since n_e decreases), as well as due to an enhancement of the negative ion loss in collisions with Ar^+ ions.

Note that the n_d-dependencies for T_{eff} and the densities of neutrals, ions and metastable atoms (Figure 6) are similar to the corresponding a_d-dependencies presented in ref.,[21] where the a_d-dependencies for neutral species were found to be in a good qualitative agreement with experimental results.

In our experiments on growth of nanoparticles,[21,29] the mass spectra for neutral species and positive ions were measured at different times during the growth cycle of nanoparticles: (i) when the nanoparticles are sufficiently small to not modify plasma properties and (ii) when the nanoparticle size and number density are large enough to strongly disturb the plasma. The dust radius for the case (ii) was found to be about 25 nm,[29] and the corresponding mass spectra are presented in Figure 1. The electrode self-bias voltage in the case (i) was larger (more than – 200 V) than that in the case (ii) (about – 100 V).[29] It was found that in the case (ii), the mass peaks of H_2 and H are respectively, 9 % and 5 % larger than the mass peaks in the case (i) whereas the mass peaks of C_2H_2, C_2H and C_4H_2 are, respectively, 15%, 14% and 9% smaller.

It was also found that the mass peaks of most ions in the plasma with large nanoparticle size and number density are smaller than the peaks for the case when dust particles do not affect much on plasma properties. In particular, the mass peaks of $C_2H_2^+$, $C_2H_3^+$, ArH^+, $C_4H_2^+$ and $C_4H_3^+$ in the case (ii) are, respectively, 25%, 20%, 55%, 26% and 19% smaller than the mass peaks in the case (i). However, the peaks at mass numbers 20 (for Ar^{++}), 38 (for Ar^+) and 76 (for $C_6H_4^+$) are, respectively, 55%, 21% and 33% larger in the case of large dust density.

Thus, the results of our calculations agree well with the experimental data. In particular, the calculated densities of C_2H_2, C_4H_2, $C_2H_3^+$, $C_4H_2^+$ and $C_4H_3^+$ are smaller and the density of Ar^+ is larger in a plasma with large dust density and size than in the dust-free case (Figure 6).

However, there is a discrepancy between the results of our calculations and the experimental data for some species (ArH^+, $C_2H_2^+$, H_2, H, C_2H and $C_6H_4^+$). This difference is due to different reactions in the mass-spectrometer (for example, the measured mass peak of C_2H originates mainly from the dissociation of C_2H_2 in the ion source of the mass spectrometer[37]). It is also because the mass spectra measurements were conducted in one

point of the plasma volume (at a height of 10 cm and a radial distance of 7 cm from the center of the powered electrode), and, therefore, the measured compositions of ions and neutrals may be different from those averaged on the plasma volume. The difference between the numerical and experimental results may also be due to various simplifications used in the model. In particular, our global model assumes that the dust particles are nearly uniformly distributed in the plasma volume, while numerous experiments show that the spatial distribution of dust particles is usually essentially inhomogeneous in dusty plasmas.[7,38] Therefore, the model here is applicable only for a qualitative analysis of Ar/C_2H_2 dusty plasmas and should be improved by inclusion of the effects of spatial nonuniformity of dust density.

Note also that in our model it is assumed that the ion temperature equals the gas temperature. Meantime, because of ion acceleration in inhomogeneous plasma regions, the spatially-averaged ion temperature is slightly larger than the gas temperature. Therefore, we checked how a deviation of the ion temperature from T_g affects the results of our calculations. We carried out our calculations for the dusty plasma case at T_i = 350 K and T_i = 450 K. The calculations were carried out assuming that T_g = 300 K, n_d =10^7 cm^{-3} and the other external conditions are the same as in Figure 6. Indeed, it was found that a variation of the ion temperature slightly affects some plasma properties. In particular, the densities of C_2H_2 and H_2 and n_e at T_i = 300 K differ by less than 1% from these densities at T_i = 350 K and T_i = 450 K. The electron temperature is also nearly independent on T_i (~3.25 eV) for the ion temperatures considered here. With increasing T_i, the dust charge Z_d slightly increases (Z_d = -81, -83 and -88e for T_i = 300, 350 and 450 K, respectively) because of decreasing the rate describing collection of positive ions of sort α by dust particles ($K_d^\alpha \approx a_d^2 \left(8\pi T_i/m_i\right)^{1/2}\left(1+\xi\tau+H\xi^2\tau^2\lambda_s n_n\sigma_{in}\right)$).[39] Here, $\tau = T_{eff}/T_i >> 1$, m_i is the ion mass, n_n is the total neutral density, $\sigma_{in} \approx 10^{-14}$ cm^2 is the cross-section for ion neutral collisions and $\xi = \left|Z_d\right| e^2 / a_d T_{eff}$. The function H satisfies $H \sim 0.1$ for $0.1 \le \beta \le 10$, $H \sim \beta$ for $\beta << 1$,

and $H \sim \beta^{-2}(\ln\beta)^3$ for $\beta >> 1$,[39] where $\beta = |Z_d| e^2 / \lambda_s T_i$, and λ_s is the screening length, which is of the same order as the Debye length.[1] Because of decreasing the rate for collection of positive ions by dust particles, the densities of positive ions are slightly increasing with an increase of T_i (for T_i = 300, 350 and 450 K, n^+_{Ar} = 4.88×10^8, 4.95×10^8 and 5.04 ×10^8 cm^{-3}, n^+_{C2H2} = 3.57×10^8, 3.59×10^8 and 3.67 ×10^8 cm^{-3}, respectively), while the density of negative ions is nearly independent on T_i (n^- ~ 1.97 ×10^7 cm^{-3}).

4. Summary and Recommendations for Developing Future Experiments

Our numerical study of an Ar/C_2H_2 plasma under typical conditions for the growth of nanoparticles has demonstrated that the densities of species taking part in the nanoparticle nucleation (negative and positive hydrocarbon ions and hydrocarbon radicals) depend on various process parameters. Accordingly, for the designing of future experiments on the controlled growth of nanoparticles in Ar/C_2H_2 plasmas, we recommend to take into account the following factors and effects:

1) Through changing the electron density, for example by varying the input power, one can enhance or suppress the production of the species taking part in the nanoparticle formation. The amount of negative ions, which are in particular assumed to be main species for the initiation of nanoparticle formation,[16] goes up with n_e (P_{abs}) for small electron densities (here, n_e < 2×10^8 cm^{-3} at P_{abs} < 5.6 W) but goes down for n_e > 2×10^8 cm^{-3}. An increase in the electron density is accompanied by a density reduction of the C_2H_2 and C_4H_2 molecules, which participate in the formation of large molecules and anions (for example, in the reaction $C_{2n}H^- + C_2H_2 \rightarrow C_{2n+2}H^- + H_2$,[23,27] where n is a natural number). Since both, the anion and hydrocarbon molecule densities, are small at large n_e (P_{abs}), an Ar/C_2H_2 plasma with low or moderate electron density is, in our opinion, more suitable for nanoparticle production than one with large n_e. It may be a

reason why most of the nanoparticle growth experiments in Ar/C_2H_2 are performed at relatively low power. [16,17,29]

2) The densities of plasma species also depend on the shape of the electron energy distribution function. The densities of C_2H^-, C_2H_2 and C_4H_2 are larger in a plasma where electrons have the Druyvesteyn energy distribution than in the case of a Maxwellian EEDF because the effective electron temperature is larger and the electron density is smaller in the former case. Therefore, in our opinion, plasmas where the EEDF is close to the Druyvesteyn distribution (for example, in capacitively coupled plasmas with f = 13.56 MHz, $n_e < 10^{11}$ cm^{-3} and $Pd > 0.2$ Torr×cm[34]) are more suitable for the production of nanoparticles.

3) Moreover, the Ar/C_2H_2 plasma properties depend on the ratio of the acetylene input flux to that of argon. The results of our study reveal that for nanoparticle growth the input flux of Q_{C2H2} should be moderate. For example, in our experiment, the optimal flux of C_2H_2 is empirically found to be around 1.5 sccm. At smaller input fluxes, the formation of nanoparticles is less probable because of small densities of C_2H^- and C_2H_2. At large Q_{C2H2}, however, the formation of particles may lack enough C_2H radicals and positive hydrocarbon ions.

4) Dust particles can essentially affect the plasma properties (Figure 6). The density of negative ions goes down with an increase of n_d due to an enhancement of the anion losses in collisions with more abundant argon ions and due to a reduced anion production through the attachment of electrons to acetylene molecules. The latter is caused by the decrease in the electron density (Figure 6a). Therefore, the growth of new nanoparticles in a plasma already containing large dust charge density $n_d|Z_d|$ should be supressed or be less intensive than in a dust-free plasma. This may be a reason why nucleation is limited to the beginning of a dust growth cycle, and hence, why the nanoparticles exhibit a monodisperse size distribution.[29] It also confirms why

new generations of nanoparticles appear in dust-free regions like the void or once the former generation has been evacuated from the plasma under the action of detrapping forces.[16,40,41]

5. Conclusion

Our numerical results have shown how the properties of an Ar/C_2H_2 plasma depend on the input power, the acetylene input flux, the shape of the electron energy distribution function and the density of nanoparticles. In particular, it has been analyzed how the process parameters affect the densities of ions and neutral species in the plasma, including the densities of species taking part in the nanoparticle nucleation. Using these analyses, recommendations on the controlled growth of nanoparticles in Ar/C_2H_2 plasmas have been formulated. It has been concluded that Ar/C_2H_2 plasmas at low discharge power, moderate input flux of acetylene and with the electron energy distribution close to the Druyvesteyn EEDF are preferable for the production of carbonaceous nanoparticles. The obtained results are relevant to many applications involving chemically-active plasmas containing impurities, especially gas discharge plasmas used for the synthesis of novel nanomaterials.

Acknowledgements: One of the authors (I. B. D.) was supported by the Humboldt Foundation. S.L., T.G. and M.M. were supported by the CNRS through PICS n°07368 and by the PHC PROCOPE project n°30790RL from Ministères des Affaires Etrangères et du Développement International (MAEDI) et de l'Education Nationale de l'Enseignement Supérieur et de la Recherche (MENESR). E. v. W. was supported in the frame of the SFB TR24 in the project B13.

Supporting Information is available from the Wiley Online Library or from the author.

Received: ; Revised: ; Published online: DOI: 10.1002/ppap.201800209

[1] *Dusty Plasmas: Physics, Chemistry, and Technological Impacts in Plasma Processing*, A. Bouchoule, Eds., Wiley, New York **1999**.

[2] I. Doğan, M. C. M. van de Sanden, *Plasma Process. Polym*. **2016**, *13*, 19.

[3] C. Arpagaus, G. Oberbossel, P. R. von Rohr, *Plasma Process. Polym*. **2018**, *15*, 1800133.

[4] K. Ostrikov, U. Cvelbar, B. Murphy, *J. Phys. D: Appl. Phys.* **2011**, *44*, 174001.

[5] L. Boufendi, M. Ch. Jouanny, E. Kovacevic, J. Berndt, M. Mikikian, *J. Phys. D: Appl. Phys.* **2011**, *44*, 174035.

[6] S. C. Wong, J. Goree, Z. Haralson, B. Liu, *Nature Physics* **2018**, *14*, 21.

[7] S. V. Vladimirov, K. Ostrikov, *Phys. Rep.* **2004**, *393,* 175.

[8] V. E. Fortov, A. V. Ivlev, S. A. Khrapak, A. G. Khrapak, G. E. Morfill, *Phys. Rep*. **2005**, *421*, 1.

[9] P. K. Shukla, B. Eliasson, *Rev. Mod. Phys*. **2009**, *81*, 25.

[10] H. Kersten, H. Deutsch, E. Stoffels, W. W. Stoffels, G. M. W. Kroesen, R. Hippler, *Contrib. Plasma Phys.* **2001**, *41*, 598.

[11] S. Hong, J. Berndt, J. Winter, *Plasma Sources Sci. Technol*. **2003**, *12*, 46.

[12] Ch. Deschenaux, A. Affolter, D. Magni, Ch. Hollenstein, P. Fayet, *J. Phys. D: Appl. Phys*. **1999**, *32*, 1876.

[13] J. Benedikt, A. Consoli, M. Schulze, A. von Keudell, *J. Phys. Chem. A* **2007**, *111*, 10453.

[14] H. C. Thejaswini, S. Peglow, U. Martens, V. Sushkov, R. Hippler, *Contrib. Plasma Phys.* **2014**, *54*, 683.

[15] H. T. Do, G. Thieme, M. Frohlich, H. Kersten, R. Hippler, *Contrib. Plasma Phys*. **2005**, *45*, 378.

[16] J. Winter, J. Berndt, S. H. Hong, E. Kovačević, I. Stefanović, O. Stepanović, *Plasma Sources Sci. Technol.* **2009**, *18*, 034010.

[17] A. P. Herrendorf, V. Sushkov, R. Hippler, *J. Appl. Phys*. **2017**, *121*, 123303.

[18] J. Berndt, E. Kovacevic, I. Stefanovic, L. Boufendi, *J. Appl. Phys*. **2009**, *106*, 063309.

[19] I. Stefanović, N. Sadeghi, J. Winter, B. Sikimić, *Plasma Sources Sci. Technol*. **2017**, *26*, 065014.

[20] Th. Wegner, A. M. Hinz, F. Faupel, T. Strunskus, H. Kersten, J. Meichsner, *Appl. Phys. Lett*. **2016**, *108*, 063108. [21] I. B. Denysenko, E. von Wahl, S. Labidi, M. Mikikian, H. Kersten, T. Gibert, E. Kovacevic, N. A. Azarenkov, *Plasma Phys. Control. Fusion* **2019**, *61*, 014014.

[22] S. Stoykov, C. Eggs, U. Kortshagen, *J. Phys. D: Appl. Phys*. **2001**, *34*, 2160.

[23] K. De Bleecker, A. Bogaerts, W. Goedheer, *Phys. Rev. E* **2006**, *73*, 026406.

[24] M. Mao, J. Benedikt, A. Consoli, A. Bogaerts, *J. Phys. D: Appl. Phys*. **2008**, *41*, 225201.

[25] D. A. Ariskin, I. V. Schweigert, A. L. Alexandrov, A. Bogaerts, F. M. Peeters, *J. Appl. Phys.* **2009**, *105*, 063305.

[26] I. V. Schweigert, A. L. Alexandrov, D. A. Ariskin, *Plasma Chem. Plasma Process*. **2014**, *34*, 671.

[27] A. Akhoundi, G. Foroutan, *Phys. Plasmas* **2017**, *24*, 053516.

[28] K. Ostrikov, H.-J. Yoon, A. E. Rider, S. V. Vladimirov, *Plasma Process. Polym*. **2007**, *4*, 27.

[29] A. M. Hinz, E. von Wahl, F. Faupel, T. Strunskus, H. Kersten, *J. Phys. D: Appl. Phys*. **2015**, *48*, 055203.

[30] A. Hurlbatt, A. R. Gibson, S. Schröter, J. Bredin, A. P. S. Foote, P. Grondein, D. O'Connell, T. Gans, *Plasma Process. Polym*. **2017**, *14*, 1600138.

[31] E. G. Thorsteinsson, J. T. Gudmundsson, *Plasma Sources Sci. Technol*. **2009**, *18*, 045001.

[32] M. A. Lieberman, A. J. Lichtenberg, *Principles of Plasma Discharges and Materials Processing* 2nd edn., Wiley, New York **2005**.

[33] J. T. Gudmundsson, *Plasma Sources Sci. Technol.* **2001**, *10*, 76.

[34] V. A. Godyak, R. B. Piejak, B. M. Alexandrovich, *Plasma Sources Sci. Technol*. **1992**, *1*, 36.

[35] I. B. Denysenko, H. Kersten, N. A. Azarenkov, *Phys. Rev. E* **2015**, *92*, 033102.

[36] I. B. Denysenko, H. Kersten, N. A. Azarenkov, *Phys. Plasmas* **2016**, *23*, 053704.

[37] http://webbook.nist.gov

[38] M. Mikikian, L. Boufendi, A. Bouchoule, H. M. Thomas, G. E. Morfill, A. P. Nefedov, V. E. Fortov, The PKE-Nefedov Team, *New J. Phys.* **2003**, *5*, 19.

[39] S. A. Khrapak, S. V. Ratynskaia, A. V. Zobnin, A. D. Usachev, V. V. Yaroshenko, M. H. Thoma, M. Kretschmer, H. Höfner, G. E. Morfill, O. F. Petrov, V. E. Fortov, *Phys. Rev. E* **2005**, *72***,** 016406.

[40] M. Hundt, P. Sadler, I. Levchenko, M. Wolter, H. Kersten, K. Ostrikov, *J. Appl. Phys.* **2011**, *109*, 123305.

[41] F. M. J. H. van de Wetering, S. Nijdam, J. Beckers, *Appl. Phys. Lett*. **2016**, *109*, 043105.

Graphical Abstract

Properties of an Ar/C_2H_2 plasma are studied using a volume-averaged model for the process conditions of our experiments on nanoparticle growth. It is analyzed how the densities of plasma species, initiating the formation of carbonaceous nanoparticles, depend on the input power, the acetylene input flux, the shape of the electron energy distribution function and the density of nanoparticles.

I. B. Denysenko*, E. von Wahl, S. Labidi, M. Mikikian, H. Kersten, T. Gibert

Effects of Process Conditions on the Chemistry of an Ar/C_2H_2 Dust-Forming Plasma